Philosophical Magazine,
Vol. 00, No. 00, DD Month 200x, 1–9

Theoretical investigation of superconductivity in ternary silicide NaAlSi with layered diamond-like structure

H. M. Tütüncü*[1,2], Ertuğrul Karaca[1], G. P. Srivastava[3]

[1]Sakarya Üniversitesi, Fen-Edebiyat Fakültesi, Fizik Bölümü, 54187, Adapazarı, Turkey

[2]Sakarya Üniversitesi, (BIMAYAM), Biyomedikal, Manyetik ve Yarıiletken Malzemeler Araştırma Merkezi, 54187, Adapazarı, Turkey

[3]School of Physics, University of Exeter, Stocker Road, Exeter EX4 4QL, UK

(Received 00 Month 200x; in final form 00 Month 200x)

We have investigated the electronic structure, phonon modes, and electron-phonon coupling to understand superconductivity in the ternary silicide NaAlSi with a layered diamond-like structure. Our electronic results, using the density functional theory within a generalized gradient approximation, indicate that the density of states at the Fermi level mainly is mainly governed by Si p states. The largest contributions to the electron-phonon coupling parameter involve Si-related vibrations both in the x-y plane as well as along the z-axis in the x-z plane. Our results indicate that this material is an s-p electron superconductor with a medium level electron-phonon coupling parameter of 0.68. Using the Allen-Dynes modification of the McMillan formula we obtain the superconducting critical temperature of 6.98 K, in excellent agreement with experimentally determined value of 7 K.

1 Introduction

Anti–PbFCl–type AFePn (A = alkali metals, Pn = P or As) compounds have been extensively studied due to their interesting magnetic and superconducting properties [1–7]. High temperature superconductivity has been discovered for LiFeAs with the superconducting transition temperature (T_c) at 18 K [1]. However, the 111 Fe-based superconductor LiFeAs [1, 5–7] contains a strong magnetic element, Fe, whose magnetic ordering weakens or interferes with the superconducting state in this material. In 2007, Kuroiwa and workers [8] succeeded in synthesizing, by high pressure technique, a new member of ternary silicide NaAlSi with a superconducting transition temperature of 7 K. This discovery is very interesting since this material is an s-p electron superconductor, with a high T_c at ambient pressure. NaAlSi has the same crystal structure as the 111 Fe-based superconductor LiFeAs [1, 5–7, 9] (anti–PbFCl–type, space group P4/nmm, Z = 2). As the magnetic metal Fe is replaced by the nonmagnetic metal Al in the ternary silicide NaAlSi, no magnetic order exists to possibly weaken or interfere with superconducting state. Kuroiwa and workers [8] have also succeeded in synthesizing the isostructural compound NaAlGe but did not observe superconductivity in this material above 1.8 K. As the electronic band structure of NaAlGe is very similar to that of NaAlSi [10, 11], Kuroiwa and workers [8] suggested that the Si-related high frequency phonon modes and/or the contribution of Si-3p electronic states play an important role in establishing the BCS-type superconductivity in ternary silicide NaAlSi. The ternary superconductor NaAlSi has also been investigated under pressure [10]. The structure remains stable up to 15 GPa. Resistivity and susceptibility measurements [10] indicate an increase of T_c up to 2 GPa, followed by a decrease until superconductivity disappears at 4.8 GPa.

Several theoretical investigations of the electronic, vibrational, and thermodynamic properties of NaAlSi have been reported. Local–density approximation calculations using the full-potential local-orbital scheme [11] have been made to investigate the electronic properties. Both all-electron full-potential linear augmented plane wave scheme and pseudopotential plane wave scheme within the generalized gradient

* Corresponding author. Email: t utuncu@sakarya.edu.tr

approximation have been employed to investigate the structural properties, The theoretical work in [12] has also presented the vibrational and thermodynamic properties of NaAlSi using the density functional theory and quasi-harmonic approximation. However, no systematic theoretical attempt has been carried out to investigate the structural, electronic, phononic and electron-phonon interaction properties of this material by employing a single scheme.

In this work we present a systematic *ab initio* investigation of the structural and electronic properties of NaAlSi by using the plane wave pseudopotential method within the generalized gradient approximation of the density functional scheme. The details of the electronic structure of both phases are similar to those described in our previous publications (see, *e.g.* [13]). We have further carried out *ab initio* linear response calculations of the lattice dynamics for NaAlSi. The calculated phonon spectrum and density of states are discussed in detail. The linear response method and the Migdal-Eliashberg approach [14–16] are used to study electron-phonon interaction. The Eliashberg function $\alpha^2\mathrm{F}(\omega)$ and the electron-phonon mass enhancement parameter λ are calculated. The Allen-Dynes modification [17,18] of the McMillan formula has been used to estimate the superconducting transition temperature T_c. Atom-resolved contributions to the electronic states near the Fermi energy and of the largest contributions to λ are analyzed to provide a clear understanding of the development of BCS-type superconductivity in this material.

2 Theory

The first-principles calculations used in this work are based on density functional theory using a plane-wave expansion of Kohn-Sham orbitals [14]. The cut-off energy of the plane-wave expansions in reciprocal space was chosen to be 60 Ryd. The exchange-correlation energy was taken into account using the generalized gradient approximation (GGA) with the Perdew-Burke-Ernzerhof (PBE) functionality [19]. The electrostatic interaction between valence electrons and ionic cores was represented by norm-conserving pseudopotentials [20]. A nonlinear core correction is included for the Na pseudopotential. The Kohn-Sham equations [21] are solved using an iterative conjugate gradient scheme to obtain the total energy of the system. Total energy calculations were performed by making the Brillouin zone (BZ) summations using the zone-centred 12×12×12 Monkhorst-Pack grid [22], giving 196 $\boldsymbol{k}$ points within an irreducible part of the Brillouin zone (IBZ). Integration over the Brillouin zone for the electronic structure and the electronic density of states for NaAlSi was performed using zone-centred 36×36×36 Monkhorst-Pack grid, producing 3610 $\boldsymbol{k}$ points in the IBZ.

Lattice dynamics of NaAlSi was studied in the framework of the harmonic approximation to the force constants and using the linear response method [14] which is performed in the QUANTUM ESPRESSO package [14]. Within this method, the second-order derivatives of the total energy such as the dynamical matrices are calculated from the static linear response of the electrons to the variation of the external potential corresponding to periodic displacements of the atoms. The screening of the electronic system in response to the displacement of the atoms are calculated in a self consistent manner. Integration up to the Fermi surface is done by using the smearing technique with the broadening parameter σ=0.007 Ry. For the Brillouin zone integration, we use the zone-centred 12×12×12 Monkhorst-Pack $\boldsymbol{k}$ mesh in the IBZ. We have calculated 18 dynamical matrices at an uniform 4x4x4 grid $\boldsymbol{q}$-points in the Brillouin zone. Then, dynamical matrices at arbitrary wave vectors were calculated by means of a Fourier deconvolution on this mesh. The method for the electron-phonon interaction has been clearly explained in our previous works [13]. We only say that the electron-phonon interaction is studied by using the *ab initio* linear response method and the Migdal-Eliashberg approach described in Refs. [13–18].

3 Results

3.1 *Structural and Electronic Properties*

NaAlSi crystallizes in the anti–PbFCl–type structure, with two formula units per primitive tetragonal unit cell is characterized with space group P4/nmm. The atomic configuration in each unit cell consists

of two Na atoms at the (2c) (0.25, 0.25, z_{Na}) position, two Al atoms at 2(a) (0.75, 0.25, 0.00) and two Si atoms at 2(c)(0.25, 0.25,z_{Si}). Thus, this structure is characterized by two lattice parameters (a and c) and two internal parameters (z_{Na} and z_{Si}). This structure, displayed in Fig. 1, can be described as a layered structure in which Na atoms are sandwiched between diamond-like sp^3-hybridized Al-Si layers.

Our calculations suggest that the nature of bonding between Na and Al-Si layers is mainly ionic, and the Al-Si layer is characterized with covalent Al-Si bonds. The Al-Si separation of 2.57 $\mathring{A}$ is larger than in the Si-Si separation of 2.35 $\mathring{A}$ in the diamond structure of Si, employing that the Al-Si covalent interaction is weaker than the Si-Si covalent interaction in the diamond structure of Si. Due to electronic charge transfer from Na atoms to the Al-Si layers, this structure can also be described as positively charged Na and negatively charged Al-Si layers stacked alternatively along the c-direction.

The total energy calculated from full structural optimizations at selected pressures versus volume relation are fitted to the Murnaghan's equation of state [23]. The obtained equilibrium lattice parameters (a and c), unit cell volume (V), internal parameters (z_{Na} and z_{Si}) and bulk modulus (B) are presented in Tab. 1, together with the previous experimental [8,9] and theoretical results [12] for comparison. The deviation of a, c and V from the recent experimental values [8] is 0.3%, 0.5% and 0.1%, respectively while the calculated internal parameters ($z_{\mathrm{Na}} = 0.636$ and $z_{\mathrm{Si}} = 0.209$) are reasonable agreement with their experimental values of [9] 0.622 and 0.223, respectively. Our GGA result for B of 38.40 GPa is in excellent agreement with a previous theoretical value of 38.69 [12], but unfortunately no experimental data is available for comparison.

Fig. 2 (a) illustrates the calculated electronic band structure of NaAlSi along selected high symmetry directions within the first Brillouin zone of the simple tetragonal lattice. The corresponding total density of states (DOS) and the partial density of states (PDOS) of each element, broken into site and angular momentum contributions, are displayed in Fig. 2 (b). Our electronic results generally coincide with those reported in previous theoretical calculations (see, *e.g.* [11]). The calculated electronic structure clearly reveals the metallic nature of NaAlSi since one band crosses the Fermi level along the Γ–M, X–Γ and Γ–Z symmetry directions. However, the valence and conduction bands are well separated from each other along the M-X symmetry direction. The two lowest valence bands in the energy interval −10.6 to −7.4 eV derive from strongly hybridized Al 3p and Si 3s states, which is indicative of covalent Al-Si interaction. These two lowest bands are separated by a forbidden gap of 1.6 eV from the upper valence bands, which are located in the energy interval of −5.8 eV to the Fermi level. The upper valence bands largely consist of hybridized Al 3s, Al 3p, Si 3s and Si 3p orbitals with a dominant contribution of the last one. However, the contribution from the 3s states of Na to the occupied bands in NaAlSi is very small. This is expected since Na atoms are in the charge state close to Na^{1+}. This means that the Na atomic layers and the Al-Si atomic layers are linked mainly by ionic interactions. Thus, the analysis based on the electronic DOS reveals that the bonding nature in ternary silicide NaAlSi is a combination of covalent, ionic and metallic bonds.

Very close to the Fermi energy lies the (doubly degenerate) electronic band along the Γ-Z symmetry direction. This crosses the Fermi energy, by dispersing from above E_F at Γ to slightly below E_F at Z. These bands split and disperse downwards along the in-plane Γ-X and Γ-M directions with different rates. A closer examination of PDOS in Fig. 2 (c) around the Fermi energy reveals that the occupied parts of these bands is essentially contributed by the Si 3p and Al 3p orbitals, with the former contribution being much more significant. The unoccupied parts of these band are, on the other hand, almost equally contributed by Al 3s, Al 3p and Si 3p orbitals, but also contain small contributions from Si 3s and Na 3s. In the immediate vicinity of E_F the largest contribution to unoccupied states comes from Si 3p orbitals. These findings are in agreement with the results presented by Rhee *et al* [11]. Our calculated value of the density of states at the Fermi level ($N(E_F)$) is 1.06 States/eV, which is in excellent agreement with the previous theoretical value of 1.01 States/eV in the work of of Rhee *et al* [11].

3.2 *Phonons and electron-phonon interaction*

According to the BCS theory, the superconducting properties of a material are governed by electrons which have energies close to Fermi level. The discussion of the PDOS suggests that Al 3p, Si 3s and Si 3p electrons are the dominant participants of the Cooper pairs. According to the the McMillan-Hopfield

expression, the electron-phonon coupling constant λ can be expressed as

$$\lambda = \frac{N(E_F) < I^2 >}{M < \omega^2 >}, \tag{1}$$

where $< I^2 >$ is the Fermi surface average of squared electron-phonon coupling interaction. Further, M is the mass of the atoms and $< \omega^2 >$ denotes the average of squared phonon frequencies. As can be seen from the above equation, a higher value of $N(E_F)$ may give rise to a higher electron-phonon coupling parameter λ. And a smaller average phonon frequency may also give rise to a higher λ. We will, therefore, discuss the phonon eigensolutions and the role of specific phonon modes in generating dominant contribution to λ.

We first discuss the atomic origin and irreducible symmetry representation of zone-centre phonon modes. The zone-center phonon mode in NaAlSi can be categorized by the irreducible representation of the point group D_{4h}(4/mmm). According to the group theoretical analysis, the symmetries of the optical phonon modes are presented as:

$$\Gamma = 3E_g + 2E_u + 2A_{2u} + 2A_{1g} + B_{1g} \tag{2}$$

where g and u modes are Raman and infrared active respectively. The one-dimensional A and B modes include atomic displacements along the z direction, while the doubly degenerate E modes represent displacements in the x-y. The frequencies of zone-center optical phonon modes are presented together with previous theoretical results by Qin *et al.* [12] in Tab. 1. This table clearly shows that the agreement between our results and previous theoretical results [12] is very good. The maximum difference between corresponding frequencies from the two works is not more than 7%. Such differences may arise from one or more of three reasons. First, we use the norm-conserving pseudopotentials in our theoretical work while ultrasoft pseudopotentials have been used in [12]. Secondly, while we have used our calculated values for the internal parameters (see Tab 1), Qin *et al.* have taken the values of internal parameters from the experimental work of Westerhaus and Schuster [9]. Thirdly, our calculated unit cell volume is slightly smaller than the corresponding unit cell volume in the work of Qin and co-workers [12] (see Tab 1).

Our electron-phonon interaction calculations suggest that all zone-centre optical phonon modes have small electron-phonon coupling parameter, except for the lowest E_g and B_{1g} phonon modes. The eigenvector representations of these phonon modes are displayed in Fig. 3. The lowest E_g is an optical mode originates from in-plane co-operative vibrations of Na ions with the AlSi layer, as seen in Fig. 3. The B_{1g} is the optical mode involving inter-layer Si-Si vibrations along the c-axis. Both these vibrational modes dynamically change the tehrahedral bond angles in $AlSi_4$, which causes overlap of Al and Si electron orbits. This overlap leads to larger electron-phonon coupling parameter for these phonons mode than other zone-centre phonon modes. The electron-phonon coupling parameters of these phonon modes are: $\lambda(E_g) = 1.22$ and $\lambda(B_{1g}) = 1.94$. Clearly, the electron-phonon interaction for these phonon modes is very strong. However, the the electron-phonon interaction involving the B_{1g} mode is one and a half times stronger than the interaction involving the E_g mode. With this in mind we can say that the combined largest displacement from both these modes is that of Si atoms. Thus, the present work reveals that Si-related vibrational phonon modes and the Si 3p electronic states are the main contributors for the development of the BCS superconducting properties of NaAlSi. This observation confirms the suggestion forwarded by Kuroiwa and co-workers [8], who mentioned that although the electronic properties of NaAlGe [8] are similar to those of NaAlSi, no sign superconductivity is found above 1.8 K for NaAlGe.

So far, we have discussed the zone-center phonon modes only. However, a complete understanding of electron-phonon coupling needs the knowledge of the complete phonon dispersion relations throughout the BZ. The calculated phonon dispersion curves along the high symmetry directions of the Brillouin zone are displayed in Fig. 4 (a). Since the primitive unit cell contains six atoms, there are 18 phonon bands, including three acoustic bands and 15 optical bands. No imaginary phonon modes in ternary silicide NaAlSi are found, confirming the dynamical stability of this material in the anti-PbFCl-type structure. The phonon branches can be divided into two parts, with a small gap of 0.5 THz due to the mass difference between different atomic mass types. The three acoustic and nine optical branches acquire the low frequency region below 7.5 THz. The acoustic branches disperse up to 4 THz. Some optical phonon branches in this region

also show considerable dispersion. The high frequency region from 8.0 to 11.95 THz is formed by six optical phonon branches. These phonon branches are dispersive along the in-plane symmetry directions Γ-X and Γ-M. However, these are less dispersive along X-M and rather totally flat along Γ-Z. The latter behavior indicates that these arise from atoms between which there is very weak interaction along the z-axis. This, in turn, suggests that the crystal structure of NaAlSi can be viewed, at least partly, as a layered structure.

The overall characteristics of the phonon dispersion relations can be understood well by studying the phonon density of states. The total and partial density of states for NaAlSi are presented in Fig. 4 (b). Although Na atoms are the lightest element in NaAlSi, the Na-related phonons are mainly confined to the frequency region below 5 THz. Thus, Na atoms contribute mainly to the acoustic and low-frequency optical branches. However, the heavier Al and Si atoms make much smaller contribution to these phonon branches. Such low frequencies of sodium vibrations indicate rather weak bonding forces between this light mass atom and other atoms. The frequency region between 5 and 6 THz is dominated by the optical vibrations of all the three atomic species. However, Na atoms remain relatively silent the frequency region above 6 THz. In the frequency region from 6 THz to 7.5 THz, the main contributions arise from Si atoms with considerable contributions of Al atoms. The frequency domain above the gap region consists of mainly stretching vibrations in the $AlSi_4$ tetrehedra due to the strong covalent bond between Al and Si atoms.

The main idea of this work is to investigate the strength of the electron-phonon interaction in NaAlSi in order to gain a clear understanding of the development of the BCS-type superconductivity in this material. To this end, we illustrate the Eliashberg function $\alpha^2F(\omega)$ and the accumulative electron-phonon coupling parameter $\lambda_{\rm accum}$ together in Fig 5. In general, the phonon frequency variation of Eliashberg function is similar to that the total phonon density of states. The accumulative electron-phonon coupling parameter $\lambda_{\rm accum}$, defined as

$$\lambda_{\rm accum}(\omega) = \int_0^\omega \lambda(\omega')\mathrm{d}\omega' = 2\int_0^\omega \frac{\alpha^2F(\omega')}{\omega'}\mathrm{d}\omega', \tag{3}$$

increases rapidly up to 6 THz and then slowly up to 10 THz when it saturates. From the knowledge of $\alpha^2F(\omega)$ we are able to calculate the average, or accumulative, electron-phonon coupling constant λ, which is a good measure of the overall strength of the electron-phonon interaction; it is given by

$$\lambda = \int \lambda(\omega)\mathrm{d}\omega = 2\int \frac{\alpha^2F(\omega)}{\omega}\mathrm{d}\omega. \tag{4}$$

The value of average electron-phonon coupling parameter is found to be 0.68, which indicates that the electron-phonon interaction is of medium strength in ternary silicide NaAlSi. This value is much smaller than the values of electron-phonon coupling parameters for the lowest E_g mode and the B_{1g} mode (see Fig 3). **In order to explain this large difference, we have shown the phonon linewidths and electron-phonon coupling parameters of these phonon modes in Fig 6. Firstly, along the Γ-M and Γ-X directions, the E_g mode splits into two phonon branches: E_g^1 and E_g^2. Secondly, the phonon linewidths and electron-phonon coupling parameters of these optical branches decrease rapidly with increasing the q wave vector along both the symmetry directions. Thus, the average electron-phonon coupling parameter becomes much smaller than the values of zone-centre electron-phonon coupling parameters for the lowest E_g mode and the B_{1g} mode. From this we can also state that the coupling of electrons is largest with the long wavelength E_g and B_{1g} modes.**

From the calculated value of average electron-phonon coupling parameter, the superconducting transition temperature T_C is calculated using the the Allen-Dynes modification of the McMillian formula [18]

$$T_C = \frac{\omega_{\ln}}{1.2}\exp\left(-\frac{1.04(1+\lambda)}{\lambda-\mu^*(1+0.62\lambda)}\right), \tag{5}$$

where the logarithmically averaged phonon frequency $\omega_{\ln}$ is defined as

$$\omega_{\ln} = \exp\left(2\lambda^{-1}\int_0^\infty \frac{\mathrm{d}\omega}{\omega}\alpha^2F(\omega)\ln\omega\right). \quad (6)$$

From the above equation, the value of $\omega_{\ln}$ is found to be 216.27 K. μ^* in Eq. 5 is the screened Coulomb pseudopotential parameter which usually takes a value between 0.10 and 0.13 [18, 24–29]. At the end, using the Allen-Dynes formula and taking typical values of μ^* = 0.10, 0.11, 0.12 and 0.13, we obtain T_c= 6.98, 6.39, 5.82 and 5.28 K, respectively. These values are in acceptable accordance with its experimental value of 7.0 K [8].

4 Summary

In this work, we have investigated the structural, electronic, vibrational, and superconducting properties of NaAlSi adopting the anti-PbFCl-type structure by using the generalized gradient approximation of the density functional theory and the planewave pseudopotential method. The calculated structural parameters are in reasonable agreement with available theoretical and experimental results. A main feature of the electronic structure is the existence of a nearly flat band along the Γ–Z direction, leading to a sharp peak in the electronic density of states, close to the Fermi level. This peak is created by the p states of Si atoms. From an analysis of the density of states the bonding can be categorized as as a mixture of metallic, ionic and covalent contributions.

This material is dynamically stable, as no instabilities in the phonon dispersion curves are found. The present work reveals that the long wavelength lowest E_g and the B_{1g} modes are most strongly coupled to electrons, with the electron-phonon interaction strengths $\lambda(E_g) = 1.22$ and $\lambda(B_{1g}) = 1.94$. The lowest E_g is an optical mode originating from in-plane co-operative vibrations of Na ions with the AlSi layer. The B_{1g} is the optical mode involving inter-layer Si-Si vibrations along the c-axis. The combined electronic structure and phonon studies clearly suggest that the main contribution to the BCS superconductivity comes from Si-related phonon modes and Si-related high density of electronic states near the Fermi energy.

From the integration of Eliashberg spectral function $\alpha^2F(\omega)$, the value of average electron-phonon coupling parameter is calculated to be 0.68. Thus, we can conclude that the ternary silicide NaAlSi is a phonon-mediated BCS superconductor with the medium electron-phonon coupling strength. Using the Allen-Dynes modified McMillian equation with the screened Coulomb pseudopotential parameter μ^* = 0.10, the value of superconducting critical temperature is found to be 6.98 K which is in excellent agreement with its experimental value of 7.0 K.

ACKNOWLEDGEMENT

The calculations were performed using the Intel Nehalem (i7) cluster (ceres) at the University of Exeter.

References

[1] J. H. Tapp, Z. Tang, Bing Lv, K. Sasmal, B. Lorenz, P. C. W. Ch u, and A. M. Guloy, Phys. Rev. B 78 (2008) p. 060505(R).
[2] X. C. Wang , Q. Q. Liu, Y. X. Lv, W. B. Gao, L. X. Yang, R. C. Yu, F. Y. Li and C. Q. Jin, Solid State Commun. 148 (2008) p. 538.
[3] Z. Deng, X. C. Wang, Q. Q. Liu, S. J. Zhang, Y. X. Lv, J. L. Zhu, R. C. Yu and C. Q. Jin, EPL 87 (2009) p. 37004. p. 37004.
[4] K. Sasmal, B. Lv, Z. J. Tang, F. Chen, Y. Y. Xue, B. Lorenz, A. M. Guloy and C. W. Chu, Phys. Rev. B 79 (2009) p. 184516.
[5] Zhi Li, J. S. Tse, and C. Q. Jin, Phys. Rev. B 80 (2009) p. 09250. 3.
[6] S. V. Borisenko, V. B. Zabolotnyy, D. V. Evtushinsky, T. K. Kim, I. V. Morozov, A. N. Yaresko, A. A. Kordyuk, G. Behr, A. Vasiliev, R. Follath, and B. Büchner, Phys. Rev. Lett. 105 (2010) p. 067002.
[7] P. M. R. Brydon, M. Daghofer, C. Timm, and Jeroen van den Brink, Phys. Rev. B 83 (2011) p. 060501(R).
[8] S. Kuroiwa, H. Kawashima, H. Kinoshita, H. Okabe and J. Akimitsu, Physica C 466 (2007) p. 11.
[9] W. Westerhaus and H. U. Schuster, Z. Naturforsch. B 34 (1979) p. 352.
[10] L. Schoop, L. Müchler, J. Schmitt, V. Ksenofontov, S. Medvedev, J. Nuss, F. Casper, M. Jansen, R. J. Cava, and C. Felser, Phys. Rev. B 86 (2012) p. 174522.
[11] H. B. Rhee, S. Banerjee, E. R. Ylvisaker, and W. E. Pickett, Phys. Rev. B 81 (2010) p. 245114.

[12] J. Qin, W. Lu, Di. Zhang and T. Fan, Physica B 407 (2012) p. 193.
[13] S. Bağcı, H. M. Tütüncü, S. Duman and G. P. Srivastava, Phys. Rev. B 81 (2010) p.144507.
[14] P. Giannozzi, S. Baroni, N. Bonini, M. Calandra, R. Car, C. Cavazzoni, D. Ceresoli, G. L. Chiarotti, M. Cococcioni, I. Dabo, A.D. Corso, S. de Gironcoli, S. Fabris, G. Fratesi, R. Gebauer, U. Gerstmann, C. Gougoussis, A. Kokalj, M. Lazzeri, L. Martin-Samos, N. Marzari, F. Mauri, R. Mazzarello, S. Paolini, A. Pasquarello, L. Paulatto, C. Sbraccia, S. Scandolo, G. Sclauzero, A.P. Seitsonen, A. Smogunov, P. Umari and R.M. Wentzcovitch, J. Phys.: Condens. Matter 21 (2009) p. 395502.)
[15] A. B. Migdal, Zh. Eksp. Teor. Fiz. 34 (1958) p. 1438.
[16] G. M. Eliashberg, Sov. Phys. JETP. 11 (1960) p. 696.
[17] P. B. Allen, Phys. Rev. B 6 (1972) p. 2577.
[18] P. B. Allen and R. C. Dynes, Phys. Rev. B 12 (1975) 905.
[19] J. P. Perdew, K. Burke, and M. Ernzerhof, Phys. Rev. Lett. 77 (1996) p. 3865.
[20] R. Stumpf, X. Gonge and M. Scheffler, A List of Separable, Norm-conserving, Ab Initio Pseudopotentials (Fritz-Haber-Institut, Berlin, 1990).
[21] W. Kohn and L. J. Sham, Phys. Rev. 140 (1965) p. A1133.
[22] H. J. Monkhorst and J. D. Pack, Phys. Rev. B 13 (1976) p. 5188.
[23] F. D. Murnaghan, Proc. Nat. Acad. Sci. USA 50 (1944) p. 697.
[24] P. Morel and P. W. Anderson, Phys. Rev. 125 (1962) p. 1263.
[25] W. L. McMillan, Phys. Rev. 167 (1968) p. 331.
[26] P. P. Singh, Phys. Rev. B 75 (2007) p. 125101.
[27] I. Errea, M. Martinez-Canales and A. Bergara, Phys. Rev. B 78 (2008) p. 172501.
[28] E. Svanidze and E. Morosan, Phys. Rev. B 85 (2012) p. 174514.
[29] B. Wiendlocha, M. J. Winiarski, M. Muras, C. Zvoriste-Walters, J.-C. Griveau, S. Heathman, M. Gazda and T. Klimczuk, Phys. Rev. B 91 (2015) p. 024509.

Table 1. Structural parameters for the simple tetragonal NaAlSi, and their comparison with available experimental and theoretical results.

Source	$a(\mathring{A})$	$c(\mathring{A})$	V($\mathring{A}^3$)	z_{Na}	z_{Si}	B(GPa)
This work	4.131	7.328	125.05	0.636	0.209	38.40
Experimental [8]	4.119	7.362	124.90			
Experimental [9]	4.135	7.379	126.17	0.622	0.223	
GGA [12]	4.136	7.354	125.80			38.69

Table 2. The calculated zone-center phonon frequencies (in THz) for ternary silicide NaAlSi and their comparison with previous GGA calculations.

Source	E_g	E_u	A_{2u}	E_g	A_{1g}	B_{1g}	E_u	A_{1g}	E_g	A_{2u}
This work	3.018	3.726	4.830	4.835	4.890	6.016	8.532	8.612	9.663	11.820
GGA [12]	2.818	3.807	4.856	4.766	4.946	5.965	8.573	8.663	9.442	11.661

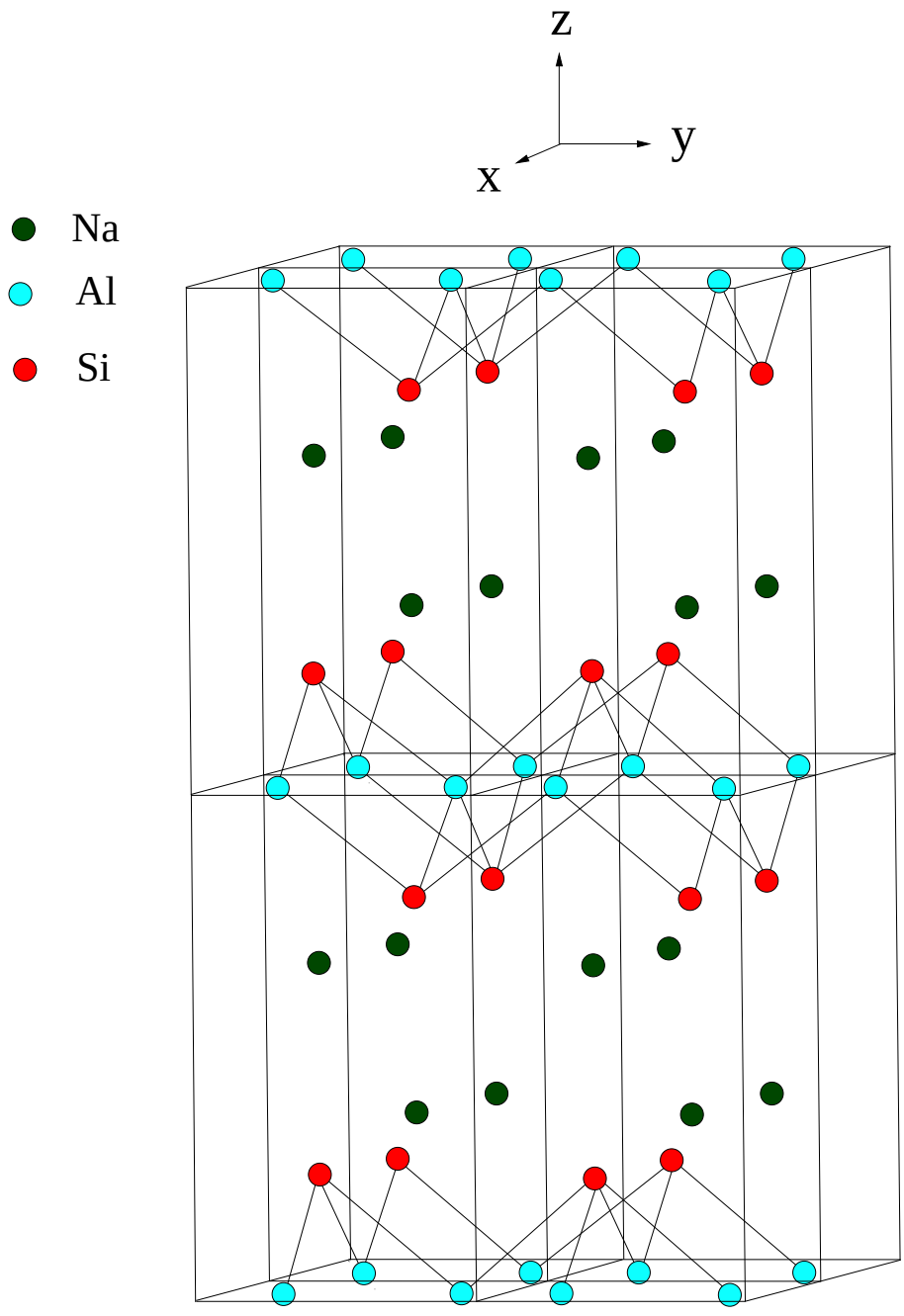

Figure 1. The crystal structure of ternary silicide NaAlSi showing Si-Al-Si layers and Na ions sheets alternatively stacked along the c-axis. **Each Al atom is tetrahedrally surrounded by four Si atoms.**

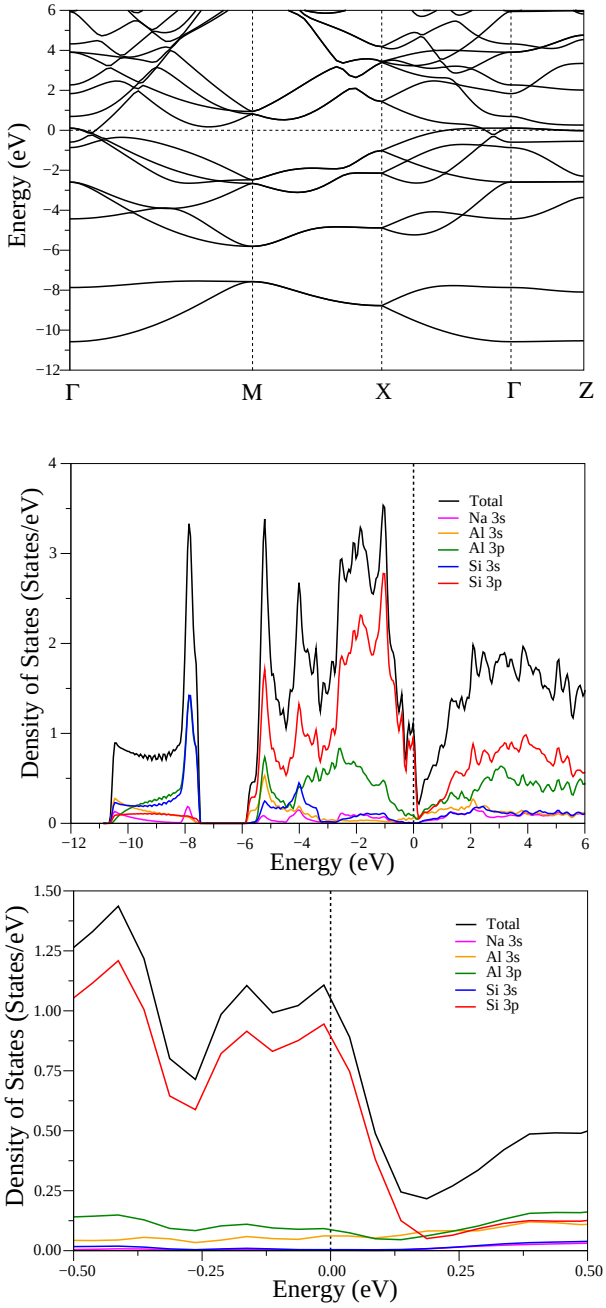

Figure 2. (a) The calculated band structure of ternary silicide NaAlSi along the high symmetry directions in the first Brillouin zone of simple tetragonal lattice. (b) The calculated total and partial density of states. (c) The calculated total and partial density of states close to the Fermi level.

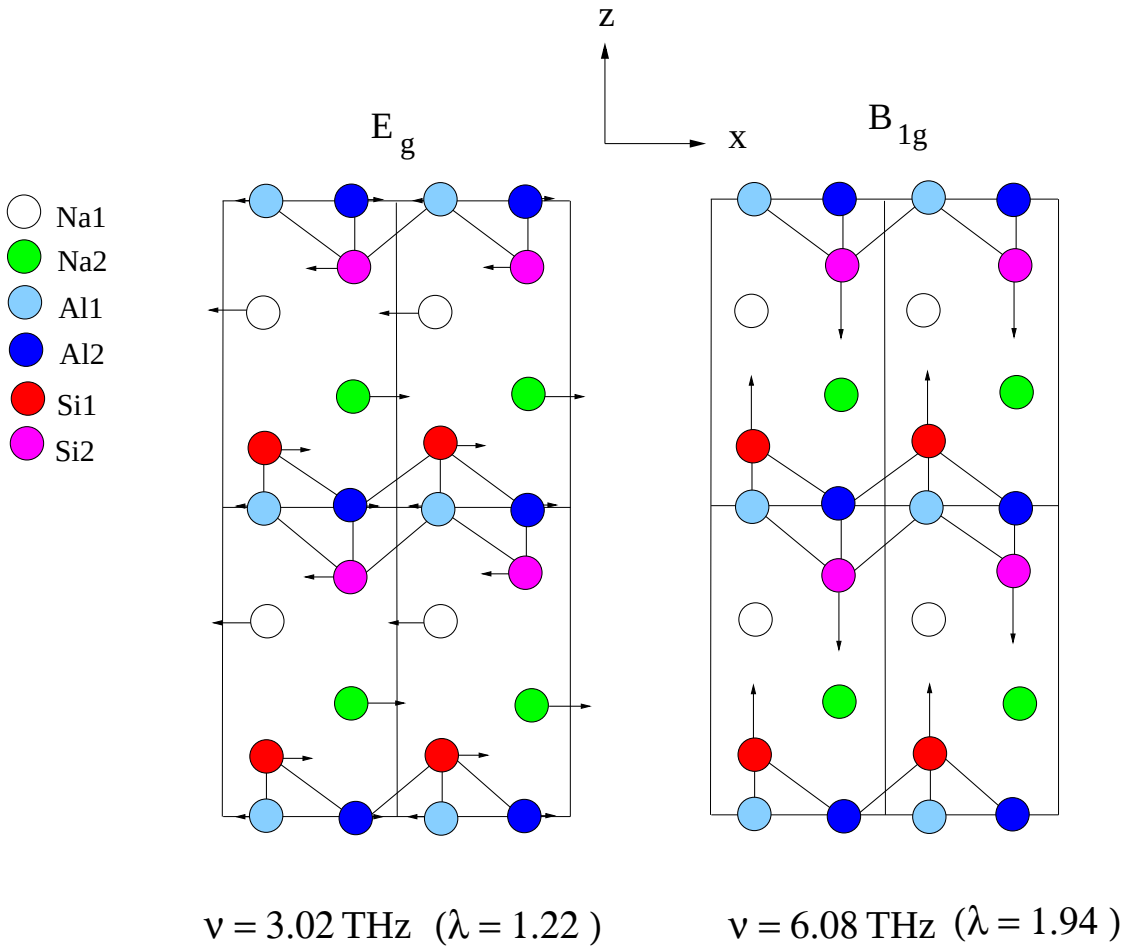

Figure 3. Eigenvector representations of the zone-centre E_g and B_{1g} phonon modes in ternary silicide NaAlSi.

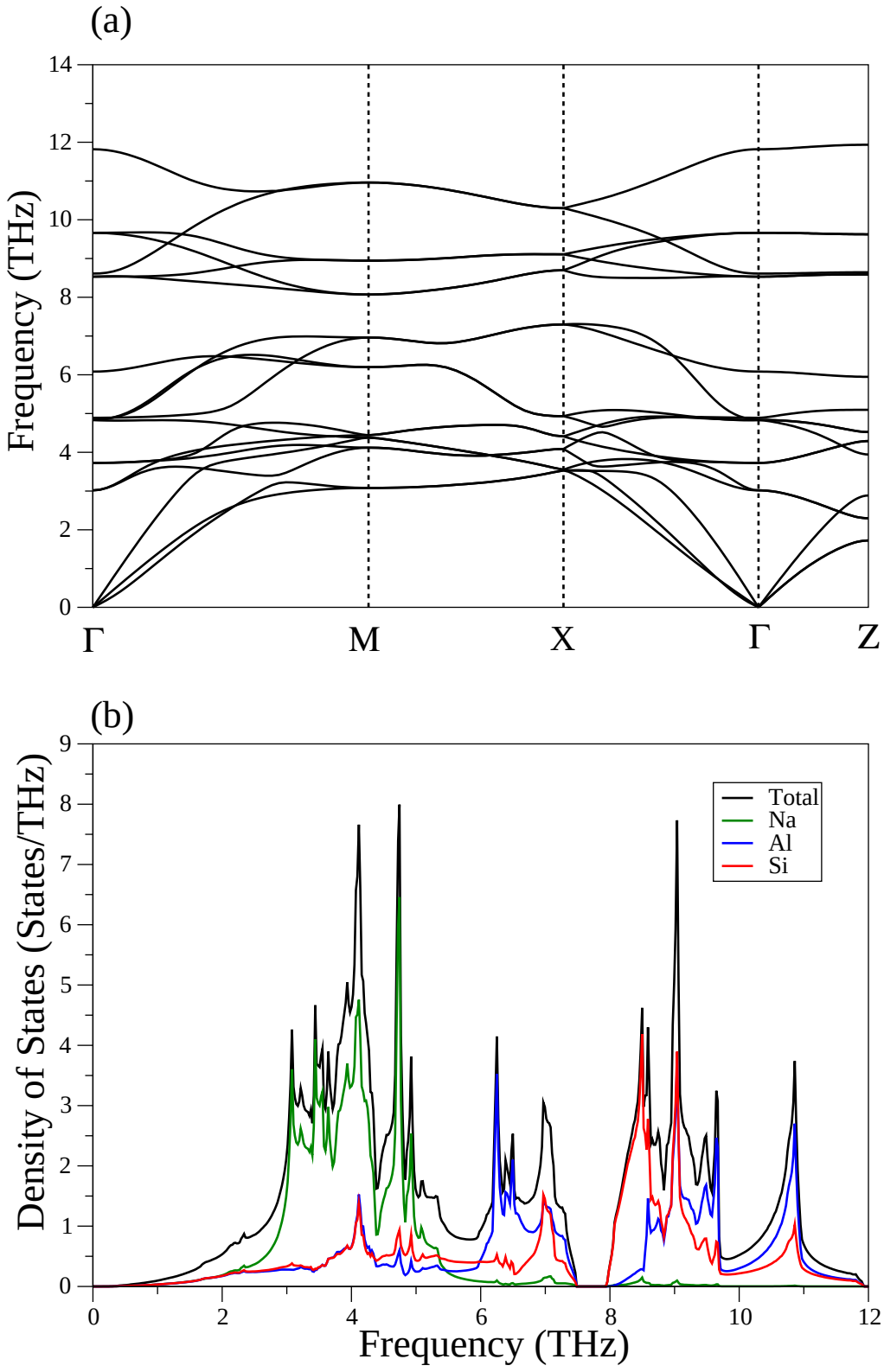

Figure 4. (a) The calculated phonon dispersion curves along high symmetry directions in the Brillouin zone for the simple tetragonal NaAlSi. (b) Total and partial phonon density of states.

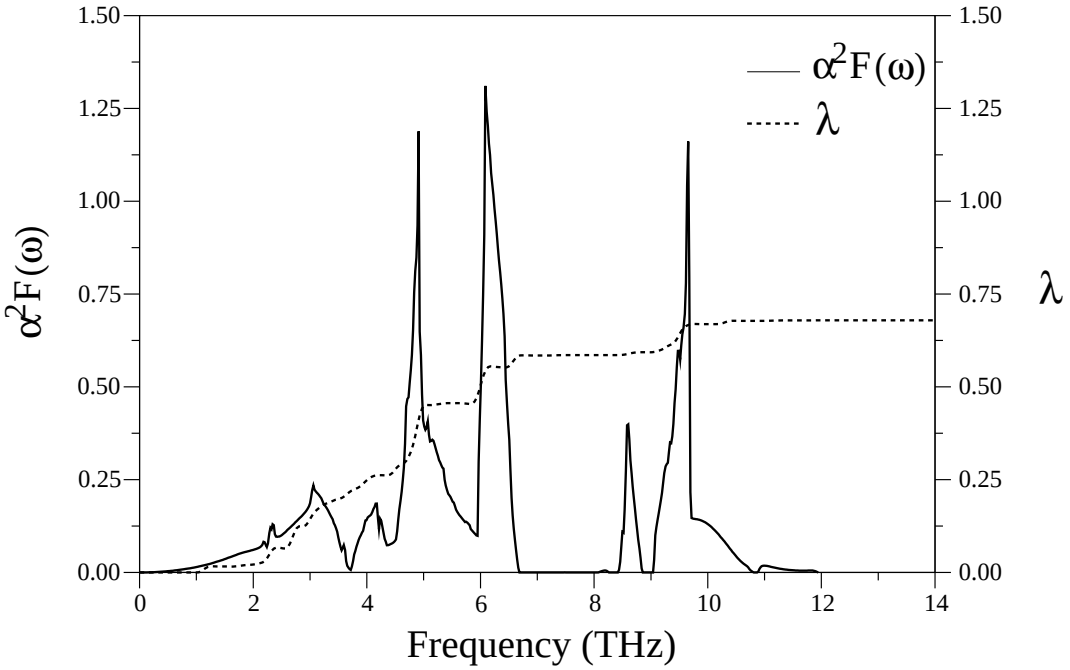

Figure 5. The calculated electron-phonon spectral function $\alpha^2F(\omega)$ (solid line) and the electron-phonon coupling parameter λ (dashed line) for ternary silicide NaAlSi.

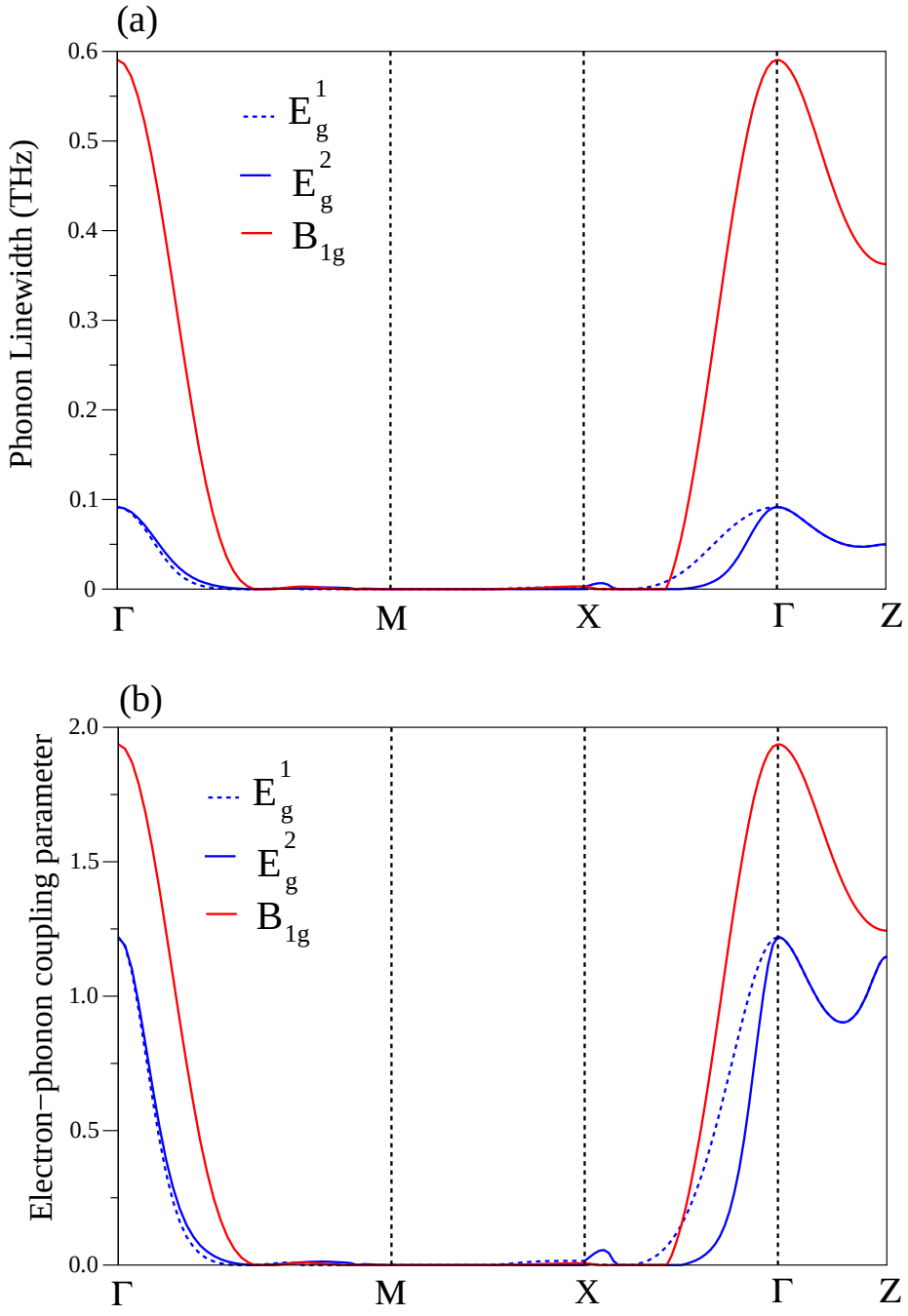

Figure 6. **(a) The calculated wavevector-dependent phonon linewidths of E_g and B_{1g} phonon modes for for ternary silicide NaAlSi.** (b) The calculated wavevector-dependent electron-phonon coupling parameters of E_g and B_{1g} phonon modes for for ternary silicide NaAlSi.